NASA TECHNICAL MEMORANDUM

NASA TM X- 62,455

NASA TM X-62,455

(NASA-TM-X-62455) THE INFLUENCE OF ENGINE/TRANSMISSION/GOVERNOR ON TILTING PROPROTOR AIRCRAFT DYNAMICS (NASA) 27 p HC $3.75 CSCL 01C

N75-28050

Unclas
G3/05 29886

THE INFLUENCE OF ENGINE/TRANSMISSION/GOVERNOR ON TILTING PROPROTOR AIRCRAFT DYNAMICS

Wayne Johnson

Ames Research Center
and
U.S. Army Air Mobility R&D Laboratory
Moffett Field, Calif. 94035

June 1975

1. Report No.	2. Government Accession No.	3. Recipient's Catalog No.
TMX-62,455		

4. Title and Subtitle	5. Report Date
The Influence of Engine/Transmission/Governor on Tilting Proprotor Aircraft Dynamics	6. Performing Organization Code
7. Author(s)	8. Performing Organization Report No.
Wayne Johnson	A-6172
9. Performing Organization Name and Address	10. Work Unit No.
Ames Research Center and U.S. Army Air Mobility R&D Laboratory Moffett Field, California 94035	505-10-22
	11. Contract or Grant No.
	13. Type of Report and Period Covered
12. Sponsoring Agency Name and Address	Technical Memorandum
National Aeronautics and Space Administration Washington, D.C. 20546	14. Sponsoring Agency Code

15. Supplementary Notes

16. Abstract

An analytical model is developed for the dynamics of a tilting proprotor aircraft engine and drive train, including a rotor speed governor and interconnect shaft. The dynamic stability of a proprotor and cantilever wing is calculated, including the engine/transmission/governor model. It is concluded that the rotor behaves much as if windmilling as far as its dynamic behavior is concerned, with some influence of the turboshaft engine inertia and damping. The interconnect shaft has a significant influence on the antisymmetric dynamics of proprotor aircraft. This report also extends the proprotor aerodynamics model to include reverse flow, and develops a refinement on the method used to calculate the kinematic pitch/bending coupling of the blade.

17. Key Words (Suggested by Author(s))	18. Distribution Statement
Tiltrotor aircraft Engine/transmission dynamics	Unlimited STAR Category - 05

19. Security Classif. (of this report)	20. Security Classif. (of this page)	21. No. of Pages	22. Price*
Unclassified	Unclassified	30	$3.75

*For sale by the National Technical Information Service, Springfield, Virginia 22151

NOMENCLATURE

a	Blade section two-dimensional lift-curve slope
C_P	Pylon damping coefficient
C_Q	Rotor torque coefficient, $Q/\rho\pi R^5\Omega^2$
I_b	Characteristic moment of inertia of blade
I_E	Engine inertia
I_P	Pylon roll inertia
k_I	Governor integral feedback gain
k_P	Governor proportional feedback gain
K_E	Engine shaft spring constant
K_I	Interconnect shaft spring constant
K_M	Rotor shaft spring constant
K_P	Pylon roll spring constant
N	Number of blades
p	Wing torsion degree of freedom
q_1	Wing vertical bending degree of freedom
q_2	Wing chordwise bending degree of freedom
Q	Rotor torque acting on hub
Q_E	Engine torque
Q_{E_1}	Engine shaft torque
Q_I	Interconnect shaft torque
Q_T	Transmission case reaction torque
Q_o	Torque transmitted to wing tip
Q_Ω	Engine damping coefficient
r_E	Engine gear ratio
r_I	Interconnect shaft gear ratio
R	Rotor radius
V	Air speed
α_p	Pylon roll degree of freedom
α_s	Shaft axes roll angle at hub
α_{s_o}	Shaft axes roll angle at wing tip
γ	Rotor Lock number

δ_P	Pylon angle of attack (0. for cruise mode)
ζ	Damping ratio, fraction of critical damping
θ_0^{com}	Collective pitch control
ρ	Air density
σ	Rotor solidity ratio
Ψ	Rotor azimuth, trim value
Ψ_d	Transmission azimuth, perturbation value
Ψ_b	Transmission azimuth, trim value
Ψ_E	Engine azimuth, trim value
Ψ_e	Engine azimuth, perturbation degree of freedom
Ψ_s	Rotor azimuth, perturbation degree of freedom
Ω	Rotor rotational speed

$\dot{(\ )}$	time derivative
$(\ )^*$	normalized quantity (divided by NI_b, as well as made dimensionless using ρ, Ω, and R)

THE INFLUENCE OF ENGINE/TRANSMISSION/GOVERNOR ON TILTING PROPROTOR AIRCRAFT DYNAMICS

Wayne Johnson*

Ames Research Center and
U.S. Army Air Mobility R&D Laboratory
Moffett Field, California

SUMMARY

An analytical model is developed for the dynamics of a tilting proprotor aircraft engine and drive train, including a rotor speed governor and interconnect shaft. The dynamic stability of a proprotor and cantilever wing is calculated, including the engine/transmission/governor model. It is concluded that the rotor behaves much as if windmilling as far as its dynamic behavior is concerned, with some influence of the turboshaft engine inertia and damping. The interconnect shaft has a significant influence on the antisymmetric dynamics of proprotor aircraft. This report also extends the proprotor aerodynamics model to include reverse flow, and develops a refinement on the method used to calculated the kinematic pitch/bending coupling of the blade.

INTRODUCTION

The rotor rotational speed perturbation ($\dot{\psi}_s$) has an important role in the dynamics of tilting proprotor aircraft, as shown in references 1 and 2. In these earlier investigations, the author considered only the two limiting cases of a windmilling rotor and constant rotor speed. However, because of the great impact of the rotor speed degree of freedom on the dynamics, a better model for this motion must be developed before proceeding to more advanced studies. This report develops an analytical model for the rotor speed dynamics, including the turboshaft engine inertia and damping, drive train flexibility, and pylon roll motion. A rotor speed governor is also included; and the interconnect shaft between the rotors, which has an important effect on antisymmetric dynamics of the vehicle.

---

*Research Scientist, Large Scale Aerodynamics Branch, NASA-Ames Research Center

This report is an extension of reference 3, which develops an analytical model for tilting proprotor aircraft dynamics. In addition to the engine/transmission/governor analysis, the proprotor aerodynamic model is extended to include reverse flow, and a method is developed for calculating the kinematic pitch/bending coupling of the rotor blades. The notation of this work follows that of reference 3.

ENGINE/TRANSMISSION MODEL

In references 1 and 2, the windmilling rotor and constant rotor speed cases were considered. For windmilling or autorotative operation, the rotor is free to turn on the shaft. No torque moments are transmitted from the rotor to the shaft, and no shaft roll motion is transmitted to the rotor. The equation of motion for the rotor speed perturbation ($\dot{\psi}_s$) is just $Q = 0$, or $C_Q/\sigma - a = 0$. There is no spring term, so the system is first order in ψ_s . The rotor azimuth perturbation ψ_s is defined with respect to the shaft axes, which have roll angle α_x ; thus the rotor speed perturbation with respect to space is $\dot{\psi}_s + \dot{\alpha}_x$.

For the constant rotor speed case, the ψ_s degree of freedom and equation of motion are dropped from the system (i.e. the appropriate row and column eliminated from the coefficient matrices). The solution for the rotor speed perturbation is just $\Delta\psi_s = 0$, so the rotation speed with respect to the shaft axes is constant at the value Ω .

We consider here a more general case, including the turboshaft engine inertia and damping, the drive train flexibility, pylon roll motion, and the interconnect shaft. The degrees of freedom in this model are: rotor rotational speed perturbation ($\Delta\dot{\psi}_s$, with respect to the pylon), engine speed perturbation ($\Delta\dot{\psi}_e$, with respect to the rotor speed), and pylon roll motion (ϕ, with respect to the wing tip). Figure 1 illustrates the model considered, showing the rotor, rotor shaft, transmission, engine, pylon, and interconnect shaft; the pylon is attached to the wing tip. Tilting proprotor aircraft have an interconnect shaft running through the wing between the

rotors, so that in the event of an engine failure the remaining engine can drive both rotors. Note that in the model we consider, the interconnect-shaft bevel gear reacts directly on the wing tip, rather than on the pylon; this distinction is not relevant unless the pylon roll degree of freedom is included. In figure 1, K_M, K_E, and K_I are the shaft torsional stiffnesses; K_p is the pylon roll stiffness at the wing tip. (The interconnect-shaft stiffness K_I is for the entire shaft, i.e. a single spring between the two transmissions. The interconnect-shaft bevel gear ratio is accounted for in the definition of K_I.) The transmission gear ratios are r_E and r_I. The engine and pylon axial moments of inertia are I_E and I_P.

Figure 2 defines the motion throughout this model. The trim rotation angles are the rotor azimuth $\Psi = \Omega t$, the transmission rotation Ψ_b, and the engine rotation Ψ_E ($\Psi_b = \Omega t$ and $\Psi_E = r_E \Omega t$ except for shaft wind-up in the springs K_M and K_E). The perturbation rotations are: rotor azimuth ψ_s, transmission ψ_d (with respect to the rotor), engine ψ_e (with respect to the rotor), and the pylon roll angle α_p (with respect to the wing tip). The angles rather than rotational speeds are used as variables since this model does introduce springs on the rotations (due to the governor and interconnect shaft). The shaft axes roll angle α_{s_0} is due to the support degrees of freedom (see reference 3), and is transmitted through the engine/transmission model to the rotor. We retain the definition of ψ_s as the perturbation of rotor azimuth with respect to the pylon, thus the shaft axes roll angle at the hub is now $\alpha_s = \alpha_{s_0} + \alpha_p$.

Figure 3 shows the torques acting throughout the system. Q is the rotor torque on the hub, which is transmitted through the engine/transmission model to the rotor support. The transmitted torque is Q_0. Note that the interconnect shaft only produces a torque for the antisymmetric motions of the aircraft. For symmetric motions, the two rotors produce a rotation of the ends of the interconnect shaft in the same direction and magnitude, so $Q_I = 0$. We shall include the interconnect shaft in the derivations then, but for symmetric motions set $K_I = 0$.

The model we are developing only influences the transmission of the rotor torque and shaft axes roll angles (Q and α_z) between the rotor hub and the rotor support (wing tip). The other hub forces and moments are not involved in this analysis. Thus the only change to the analysis of reference 3 is the addition of equations of motion for the degrees of freedom $\Delta\psi_s$, ψ_e, and α_p. Specifically, we retain the concept of the interface between the rotor and support systems occuring at the rotor hub, since translation of the engine/transmission model along the z axis (the shaft) is irrelevant.

Balance of the perturbation torques throught the model gives the following relations:

rotor shaft: $$Q = k_M \Delta\psi_d$$

transmission: $$Q + Q_{E_1} r_E + Q_\Sigma r_\Sigma = 0$$
$$r_E Q_T = (r_E + 1) Q - (r_E - r_\Sigma) Q_\Sigma$$

interconnect shaft: $$Q_\Sigma = 2 k_\Sigma (-\alpha_{z_0} - \alpha_p + r_\Sigma (\psi_s + \Delta\psi_d))$$
($K_I = 0$ for symmetric motion)

engine shaft: $$Q_{E_1} = k_E (r_E \Delta\psi_d - \psi_e)$$

engine dynamics: $$I_E (\ddot{\psi}_e + r_E \ddot{\psi}_s - \ddot{\alpha}_{z_0} - \ddot{\alpha}_p) + Q_\Omega (\dot{\psi}_e + r_E \dot{\psi}_s - \dot{\alpha}_{z_0} - \dot{\alpha}_p) = Q_{E_1}$$

pylon roll: $$I_p (\ddot{\alpha}_p + \ddot{\alpha}_{z_0}) + I_E (\ddot{\alpha}_p + \ddot{\alpha}_{z_0} - \ddot{\psi}_e - r_E \ddot{\psi}_s) + k_p \alpha_p = -Q$$

pylon flexibility: $$Q_e = Q + I_p (\ddot{\alpha}_p + \ddot{\alpha}_{z_0}) + I_E (\ddot{\alpha}_p + \ddot{\alpha}_{z_0} - \ddot{\psi}_e - r_E \ddot{\psi}_s)$$

Now eliminating Q_{Σ_1} and $\Delta\psi_d$, we have

$$Q_{E_1} = \frac{1}{k_M + r_E^2 k_E + 2 r_\Sigma^2 k_\Sigma} \left\{ \begin{array}{l} -(k_M + 2 r_\Sigma^2 k_\Sigma) k_E \psi_e \\ \quad + 2 r_\Sigma k_\Sigma r_E k_E (\alpha_{z_0} + \alpha_p) \\ \quad - 2 r_\Sigma^2 k_\Sigma r_E k_E \psi_s \end{array} \right\}$$

and

$$Q = -\frac{k_M r_E}{k_M + 2r_\Sigma^2 k_\Sigma} Q_{E_1} + \frac{k_M 2 r_\Sigma k_\Sigma}{k_M + 2r_\Sigma^2 k_\Sigma} (\alpha_{z_0} + \alpha_\phi) - \frac{k_M 2 r_\Sigma^2 k_\Sigma}{k_M + 2r_\Sigma^2 k_\Sigma} \Psi_s$$

Thus the equations of motion are:

Ψ_s equation:

$$Q = -\frac{k_M r_E}{k_M + 2r_\Sigma^2 k_\Sigma} \left\{ \begin{array}{l} I_E (r_E \ddot{\Psi}_s + \ddot{\Psi}_e - \ddot{\alpha}_{z_0} - \ddot{\alpha}_\phi) \\ + Q_{S\Sigma} (r_E \dot{\Psi}_s + \dot{\Psi}_e - \dot{\alpha}_{z_0} - \dot{\alpha}_\phi) \end{array} \right\} - \frac{k_M 2 r_\Sigma^2 k_\Sigma}{k_M + 2r_\Sigma^2 k_\Sigma} \Psi_s + \frac{k_M 2 r_\Sigma k_\Sigma}{k_M + 2r_\Sigma^2 k_\Sigma} (\alpha_{z_0} + \alpha_\phi)$$

Ψ_e equation:

$$I_E (\ddot{\Psi}_e + r_E \ddot{\Psi}_s - \ddot{\alpha}_{z_0} - \ddot{\alpha}_\phi) + Q_{S\Sigma} (r_E \dot{\Psi}_s + \dot{\Psi}_e - \dot{\alpha}_{z_0} - \dot{\alpha}_\phi) + \frac{(k_M + 2r_\Sigma^2 k_\Sigma) k_E}{k_M + r_E^2 k_E + 2r_\Sigma^2 k_\Sigma} \Psi_e - \frac{2 r_\Sigma k_\Sigma r_E k_E}{k_M + r_E^2 k_E + 2r_\Sigma^2 k_\Sigma} (\alpha_{z_0} + \alpha_\phi) + \frac{2 r_\Sigma^2 k_\Sigma r_E k_E}{k_M + r_E^2 k_E + 2r_\Sigma^2 k_\Sigma} \Psi_s = 0$$

α_ϕ equation:

$$(I_\phi + I_E)(\ddot{\alpha}_\phi + \ddot{\alpha}_{z_0}) - I_E (\ddot{\Psi}_e + r_E \ddot{\Psi}_s) + k_\phi \alpha_\phi = -Q$$

shaft motion transmitted: $\alpha_z = \alpha_{z_0} + \alpha_\phi$

torque transmitted: $Q_0 = Q + (I_\phi + I_E)(\ddot{\alpha}_\phi + \ddot{\alpha}_{z_0}) - I_E (\ddot{\Psi}_e + r_E \ddot{\Psi}_s)$

We shall assume that the engine and pylon inertia are included in the inertia of the rotor support. Then we may use simply $Q_o = Q$. We shall also add pylon roll structural damping, $C_p^* = C_p/NI_b\Omega$ to the α_p equation ($\frac{1}{2}$ to $1\frac{1}{2}$% critical damping is typical).

Following reference 3, the equations are normalized by dividing by NI_b (N = number of blades, I_b = characteristic moment of inertia of the blade); and the variables are also made dimensionless using ρ, Ω, and R (the air density, rotor rotational speed, and rotor radius). Thus the equations of motion for the engine and transmission model are:

Ψ_s equation:

$$\gamma \frac{C_Q}{\sigma a} = -\frac{K_M^* r_E}{K_{MX}^*}\left\{ I_E^* (r_E \ddot{\Psi}_s + \ddot{\Psi}_e - \ddot{\alpha}_{z_o} - \ddot{\alpha}_p) + Q_\Omega^* (r_E \dot{\Psi}_s + \dot{\Psi}_e - \dot{\alpha}_{z_o} - \dot{\alpha}_p)\right\}$$
$$- \frac{K_M^* 2 r_X^2 K_X^*}{K_{MX}^*} \Psi_s + \frac{K_M^* 2 r_X K_X^*}{K_{MX}^*} (\alpha_{z_o} + \alpha_p)$$

Ψ_e equation

$$I_E^* (\ddot{\Psi}_e + r_E \ddot{\Psi}_s - \ddot{\alpha}_{z_o} - \ddot{\alpha}_p) + Q_\Omega^* (\dot{\Psi}_e + r_E \dot{\Psi}_s - \dot{\alpha}_{z_o} - \dot{\alpha}_p)$$
$$+ \frac{K_{MX}^* K_E^*}{K_{MEX}^*} \Psi_e - \frac{r_E K_E^* 2 r_X K_X^*}{K_{MEX}^*} (\alpha_{z_o} + \alpha_p)$$
$$+ \frac{r_E K_E^* 2 r_X^2 K_X^*}{K_{MEX}^*} \Psi_s = 0$$

α_p equation:

$$(I_p^* + I_E^*)(\ddot{\alpha}_p + \ddot{\alpha}_{z_o}) - I_E^* (\ddot{\Psi}_e + r_E \ddot{\Psi}_s)$$
$$+ C_p^* \dot{\alpha}_p + K_p^* \alpha_p = -\gamma \frac{C_Q}{\sigma a}$$

shaft motion transmitted: $\alpha_2 = \alpha_{2_0} + \alpha_p$

torque transmitted: $Q_o = Q$

where

$$I_E^* = I_E / N I_b$$
$$I_p^* = I_p / N I_b$$
$$K_M^* = k_M / N I_b \Omega^2$$
$$K_I^* = k_I / N I_b \Omega^2$$
$$K_E^* = k_E / N I_b \Omega^2$$
$$K_p^* = k_p / N I_b \Omega^2$$

$$K_{M_I}^* = K_M^* + 2 r_I^2 K_I^*$$
$$K_{M_{EI}}^* = K_M^* + r_E^2 K_E^* + 2 r_I^2 K_I^*$$

The turboshaft engine damping is approximately related to the engine operating condition by

$$\Omega_\Omega = \frac{\partial Q_E}{\partial \Omega_E} \cong \frac{Q_{E_o}}{\Omega_{E_o}} = \frac{P_{rotor}}{r_E^2 \Omega_{rotor}^2}$$

This approximation is based on dimensional analysis, engine theory, and turboshaft engine data (references 5 and 6). In coefficient form then:

$$\Omega_\Omega^* = \frac{\Omega_\Omega}{N I_b \Omega} = \frac{1}{r_E^2} \left(\delta \frac{C_Q}{\sigma a} \right)_{trim}$$

where $C_{Q_{trim}}$ is the trim rotor torque or power coefficient. This engine damping is typically small compared to the proprotor aerodynamic rotational damping in cruise flight. The engine inertia is generally more important.

For the windmilling case, we simply set $I_E^* = Q_\Omega^* = 0$, and drop the ψ_e and α_p degrees of freedom from the system. For the constant rotor speed case, all three degrees of freedom ψ_e, ψ_s and α_p and their equations are dropped. This model also may treat the engine out case, for which there is no engine damping, by setting $Q_\Omega^* = 0$.

The complete model developed here includes the rotor speed, engine speed, and pylon roll degrees of freedom (ψ_s, ψ_e, α_p). We shall find however that ψ_e and α_p are not very important to the dynamics. For antisymmetric motion of the aircraft, the interconnect shaft is included; for symmetric motions, $K_I = 0$. A rotor speed governor is also included, for symmetric motions only (as discussed in the next section). Note that the ψ_s equation is first order (no spring term) except for the antisymmetric case (which introduces the interconnect-shaft spring), or when the governor is included (which gives a weak spring on the rotor speed for symmetric motions also).

ROTOR SPEED GOVERNOR

We consider a rotor speed governor using integral plus proportional feedback of the rotor speed error (ε) to rotor collective:

$$\Delta\theta_0^{com} = k_I \int^\tau \varepsilon \, d\tau + k_p \varepsilon$$

The proportional gain K_p is for helicopter mode operation, to increase the rotor rotational damping in low inflow; it is programmed with nacelle tilt angle δ_p so that $K_p = 0$ in proprotor cruise mode ($\delta_p = 0$).

Assume that the sensor measures the inertial angular velocity at the center of the interconnect shaft in the fuselage; then, using the equations of motion, the rotor speed error is

$$\varepsilon = \dot\psi_s + \dot\psi_b - \frac{\dot\alpha_{\beta_0}}{r_I} - \frac{\dot\alpha_p}{r_I}$$

$$= \dot\psi_b + \frac{r_E K_E^*}{K_M^* + r_E^2 K_E^*}\dot\psi_e - \frac{1}{r_I}(\dot\alpha_{\beta_0} + \dot\alpha_p)$$

For typical transmission gear ratios, the last terms in Σ are only a few percent of $\dot{\Psi}_s$. Thus we assume for now that the governor measures the rotor speed perturbation directly, $\Sigma = \dot{\Psi}_s$, so

$$\Delta\theta_0^{com} = K_I \Psi_s + K_\phi \dot{\Psi}_s$$

This is the governor model for use with the rotor and cantilever wing analysis of reference 3. With a complete aircraft model the exact expression for Σ could be used, but in general $\Sigma = \dot{\Psi}_s$ is close.

Since the rotor speed error is measured at the center of the interconnect shaft, the governor acts only for symmetric motions of the aircraft. Note that the governor integral feedback adds a spring to the Ψ_s equation, although we will find that it is very weak.

An elementary analysis of the governor and rotor speed dynamics is possible, following reference 2. The uncoupled equation for Ψ_s is

$$I_0^* \ddot{\Psi}_s + \gamma Q_\zeta \dot{\Psi}_s = -\gamma Q_\theta \theta_0$$

where Q_ζ and Q_θ are the aerodynamic torques on the rotor. The eigenvalue of the rotor speed mode, with no governor, is then

$$s = -\gamma Q_\zeta / I_0^* \cong -\frac{\gamma \lambda \sin\phi}{C}$$

(ϕ is the inflow angle at 3/4 radius, $\tan\phi = \lambda/r_0$; see reference 2). The governor equation for cruise mode is $\theta_0 = K_I \Psi_s$, so

$$I_0^* \ddot{\Psi}_s + \gamma Q_\zeta \dot{\Psi}_s + K_I \gamma Q_\theta \Psi_s = 0$$

Then since K_I is small (of the order .02), the roots are

$$s \cong -\frac{\gamma Q_\zeta}{I_0^*} + K_I \frac{Q_\theta}{Q_\zeta}$$

and

$$s \cong -K_I \frac{Q_\theta}{Q_\zeta} \cong -K_I \frac{2}{\sin 2\phi} = -K_I \left(\frac{4\lambda}{\lambda^2} + \frac{\lambda}{4\lambda}\right)$$

These are quite good approximations to the governor and rotor speed roots. The governor adds a very small real root (long time constant) to the system, and decreases slightly the magnitude of the rotor speed root.

REVERSE FLOW

Before examining the influence of the engine/transmission/governor on the proprotor dynamics, two extensions to the analysis of reference 3 will be developed. The first extension is the incorporation of reverse flow in the aerodynamic model, which requires only some modifications to the pitch moments on the blade. By considering high inflow, the effects of reverse flow (mainly a matter of some sign changes in the reverse flow region) have automattically been included in the lift and drag forces. For example, the blade normal force in reference 3 is

$$\frac{F_z}{ac} = U\left(u_T \frac{c_l}{a_c} - u_P \frac{c_d}{a_c}\right)$$

where $U = \sqrt{u_T^2 + u_P^2}$ and $\alpha = \theta - \tan^{-1} u_P/u_T$. For low inflow these reduce to

$$\frac{F_z}{ac} \cong \tfrac{1}{2} |u_T| u_T \alpha$$

since $U \cong |u_T|$ and $\alpha \cong \theta - u_P/u_T$. The absolute value on u_T is the reverse flow influence, included automatically by the use of $U = \sqrt{u_T^2 + u_P^2}$. The aerodynamic pitch moment expressions of reference 3 require some revision however.

Including reverse flow effects, the aerodynamic pitch moment about the elastic axis is now

$$\frac{M_a}{ac} = -x_{Ae} U^2 \frac{c_l}{2a} + U^2 \frac{c c_{m_{AC}}}{2a} + \frac{M_{US}}{ac}$$

where x_A is the distance the aerodynamic center is behind the elastic axis, $c_{m_{AC}}$ is the moment coefficient about the aerodynamic center, and M_{US} is the unsteady moment; and

$$x_{Ae} = \begin{cases} x_A & \text{normal flow} \\ -\left(x_A + \frac{c}{2}\right) & \text{reverse flow} \end{cases}$$

The unsteady aerodynamic moment is:

$$\frac{M_{US}}{ac} = -\frac{c^2}{32}\left[|v|B \left(1 + 8\frac{x_{Ae}}{c} + 16\left(\frac{x_{Ae}}{c}\right)^2\right) + \left(\dot{w} + u_R w''\right)\left(1 + 4\frac{x_{Ae}}{c}\right)\right]$$

where w is the upwash velocity normal to the blade surface ($w = u_T \sin\theta - u_P \cos\theta$), $B = \partial w / \partial x$ (mainly the pitch rate $\dot{\theta}$), and $V = u_T \cos\theta + u_P \sin\theta$. For stalled flow, the unsteady moment is set to zero, $M_{US} = 0$.

Thus the only change to reference 3 is in the aerodynamic coefficients of the pitch/torsion equations of motion (pp. 89-90 of reference 3). The AC-EA offset x_A in the derivatives M_{a_T}, M_{a_P}, and M_{a_θ} is replaced by the effective offset x_{A_e}; and there are additional sign changes in the unsteady aerodynamic moments. Including reverse flow, the aerodynamic coefficients are now:

$$M_{pk_P} = \int_{r_{FA}}^{1} \left[\xi_k M_{a_T} - (F_{x_T} \vec{i}_B + F_{z_T} \vec{k}_B) \cdot \vec{Y}_{A_k} \right] dr$$

$$M_{pk_{\dot{\xi}}} = \int_{r_{FA}}^{1} \left[\xi_k M_{a_T} - (F_{x_T} \vec{i}_B + F_{z_T} \vec{k}_B) \cdot \vec{Y}_{A_k} \right] r\, dr - \int_{r_{FA}}^{1} \xi_k \frac{c^2}{32} \left(1 + 4\frac{x_{A_e}}{c}\right) 2 u_R \sin\theta\, dr$$

$$M_{pk_\zeta} = \mu \cos\psi_m M_{pk_P} + \int_{r_{FA}}^{1} \xi_k \frac{c^2}{32} \left(1 + 4\frac{x_{A_e}}{c}\right) \mu \sin\psi_m \sin\theta\, dr$$

$$M_{pk_\lambda} = \int_{r_{FA}}^{1} \left[\xi_k M_{a_P} - (F_{x_P} \vec{i}_B + F_{z_P} \vec{k}_B) \cdot \vec{Y}_{A_k} \right] dr$$

$$M_{pk_{\dot{\beta}}} = \int_{r_{FA}}^{1} \left[\xi_k M_{a_P} - (F_{x_P} \vec{i}_B + F_{z_P} \vec{k}_B) \cdot \vec{Y}_{A_k} \right] r\, dr + \int_{r_{FA}}^{1} \xi_k \frac{c^2}{32} \left(1 + 4\frac{x_{A_e}}{c}\right) 2 u_R \cos\theta\, dr$$

$$M_{pk_\beta} = \mu \cos\psi_m M_{pk_\lambda} - \int_{r_{FA}}^{1} \xi_k \frac{c^2}{32} |V| \left(1 + 8\frac{x_{A_e}}{c} + 16\left(\frac{x_{A_e}}{c}\right)^2\right) dr - \int_{r_{FA}}^{1} \xi_k \frac{c^2}{32} \left(1 + 4\frac{x_{A_e}}{c}\right) \mu \sin\psi_m \cos\theta\, dr$$

$$M_{PK\dot{q}i} = \int_{r_{FA}}^{1} \left[\xi_K M_{aT} - (F_{xT}\vec{i}_B + F_{zT}\vec{k}_B)\cdot\vec{X}_{AK} \right] \vec{k}_B \cdot \vec{\eta}_i \, dr$$
$$+ \int_{r_{FA}}^{1} \left[\xi_K M_{aP} - (F_{xP}\vec{i}_B + F_{zP}\vec{k}_B)\cdot\vec{X}_{AK} \right] \vec{i}_B \cdot \vec{\eta}_i \, dr$$
$$+ \int_{r_{FA}}^{1} \xi_K \frac{c^2}{32} \left(1 + 4\frac{\chi_{Ac}}{c}\right) 2\mu_R \vec{i}\cdot\vec{\eta}_i^{*} \, dr$$

$$M_{PKq_i} = \mu\cos\psi_m \left\{ \int_{r_{FA}}^{1} \left[\xi_K M_{aT} - (F_{xT}\vec{i}_B + F_{zT}\vec{k}_B)\cdot\vec{X}_{AK} \right] \vec{k}_B \cdot \vec{\eta}_i^{v} \, dr \right.$$
$$\left. + \int_{r_{FA}}^{1} \left[\xi_K M_{aP} - (F_{xP}\vec{i}_B + F_{zP}\vec{k}_B)\cdot\vec{X}_{AK} \right] \vec{i}_B \cdot \vec{\eta}_i^{v} \, dr \right\}$$
$$- \int_{r_{FA}}^{1} \left(\frac{F_x}{ac}\vec{i}_B + \frac{F_z}{ac}\vec{k}_B \right)\cdot\vec{X}_{AK} q_i \, dr$$
$$- \int_{r_{FA}}^{1} \xi_K \frac{c^2}{32} |V| \left(1 + 8\frac{\chi_{Ac}}{c} + 16\left(\frac{\chi_{Ac}}{c}\right)^2\right) \vec{i}_B \cdot \vec{\eta}_i^{v} \, dr$$
$$- \int_{r_{FA}}^{1} \xi_K \frac{c^2}{32} \left(1 + 4\frac{\chi_{Ac}}{c}\right) \left(\mu \sin\psi_m \vec{i}\cdot\vec{\eta}_i^{v} - (\mu\cos\psi_m)^2 \vec{i}\cdot\vec{\eta}_i^{vv}\right) dr$$

$$M_{PK\dot{P}i} = \int_{r_{FA}}^{1} \left[\xi_K M_{a\Theta} - (F_{x\Theta}\vec{i}_B + F_{z\Theta}\vec{k}_B)\cdot\vec{X}_{AK} \right] \xi_i \, dr$$
$$- \int_{r_{FA}}^{1} \xi_K \frac{c^2}{32} \mu_R \left[\xi_i^{v} V + 2\xi_i \cos\Theta \right] \left(1 + 4\frac{\chi_{Ac}}{c}\right) dr$$

$$M_{PK\dot{P}i} = -\int_{r_{FA}}^{1} \xi_K \xi_i \frac{c^2}{16} \left[|V| \left(\frac{1}{2} + 4\frac{\chi_{Ac}}{c} + 8\left(\frac{\chi_{Ac}}{c}\right)^2\right) \right.$$
$$\left. + V\left(\frac{1}{2} + 2\frac{\chi_{Ac}}{c}\right) \right] dr$$

PITCH/BENDING COUPLING

The second extension of reference 3 we consider is a method for calculating the kinematic pitch/bending coupling K_{P_i}. The definition of K_{P_i} is the rigid pitch motion due to a unit deflection of the i-th bending mode:

$$K_{P_i} = \frac{\partial \theta}{\partial q_i}$$

(For an articulated rotor, the first "bending" modes are rigid lag and flap motion about the hinges.) It is possible to simply input the kinematic coupling parameters to the stability calculations, if values are available from either measurements or some other analysis. It is also desirable however to be able to calculate the coupling from a model of the blade root geometry.

Figure 4 is a schematic of the blade root and control system geometry we consider, showing the position of the pitch bearing, pitch horn, and pitch link for no bending deflection of the blade. The radial locations of the pitch bearing and pitch link are r_{FA} and r_{PH}; the lengths of the pitch horn and pitch link are x_{PH} and x_{PL}. The orientation of the pitch horn and pitch link are given by the angles $\phi_{PH} + \theta_{.75}$ and ϕ_{PL}. Control input produces a vertical motion of the bottom of the pitch link, and hence a feathering motion of the blade about the pitch axis.

Bending motion of the blade, with either bending flexibility or an actual hinge inboard of the pitch bearing, produces an inplane or out-of-plane deflection of the pitch bearing. With the bottom of the pitch link fixed in space, a pitch change in the blade results. The vertical and inplane displacements of the pitch horn (the end at r_{PH}) due to bending of the blade in the i-th mode are:

$$\Delta z = q_i \vec{k}_B \cdot \left(\vec{\eta}_i(r_{FA}) - \vec{\eta}_i'(r_{FA})(r_{FA} - r_{PH}) \right)$$

$$\Delta x = -q_i \vec{i}_B \cdot \left(\vec{\eta}_i(r_{FA}) - \vec{\eta}_i'(r_{FA})(r_{FA} - r_{PH}) \right)$$

The kinematic pitch/bending coupling is derived from the geometric constraint

that the lengths of the pitch horn and pitch link are fixed. The result is:

$$k_{P_i} = \frac{(\cos\phi_{PL}\,\vec{i}_R + \sin\phi_{PL}\,\vec{k}_R)\cdot(\vec{\eta}_i(r_{FA}) - \vec{\eta}_i'(r_{FA})(r_{FA} - r_{PH}))}{-x_{PH}\cos(\phi_{PH} + \theta_{.75} + \phi_{PL})}$$

Similarly, for a gimballed rotor the pitch/gimbal coupling is:

$$k_{P_G} = \frac{-(r_{PH}/x_{PH})\cos\phi_{PL}}{\cos(\phi_{PH} + \theta_{.75} + \phi_{PL})} = \frac{(k_{P_G})_{\text{pitch horn horizontal}}}{\cos(\phi_{PH} + \theta_{.75} + \phi_{PL})}$$

INFLUENCE OF ENGINE/TRANSMISSION/GOVERNOR DYNAMICS

Finally, we shall examine the influence of the engine, transmission, and governor on the proprotor dynamic behavior. The case considered is a gimballed rotor operating in high inflow axial flight on a cantilever wing; this is one of the cases treated in reference 1. The degrees of freedom used are: gimbal pitch and yaw; two bending modes and the rigid pitch mode per blade; rotor speed perturbation; and wing vertical bending, chordwise bending, and torsion. For the standard case here, the ψ_e and α_p degrees of freedom, the governor, and the interconnect shaft are not included. For the dynamic behavior we consider the eigenvalues of the engine/transmission model, given in Table 1, and the damping ratios of the three wing modes, given in figures 5 through 8. Table 1 also presents the rms gust response of the rotor and wing degrees of freedom, due to random excitation by all three gust components. The gust response is nondimensional, and normalized by the gust rms magnitude; only the relative values among the various cases are of concern here. A number of cases are considered, demonstrating the impact of various model elements on the system dynamic characteristics. While the discussion may center on the figures (i.e. on the wing mode stability), the conclusions are based on comparisons of the roots and gust response as well.

For our examples we consider the 7.42 m diameter gimballed rotor described in reference 1. This rotor is designed for 29000 N. hover thrust at a rotor speed of 48 rad/sec, powered by a Lycoming LTC1K-4K engine (modified T53-L-13B). The numbers used for the engine and transmission are:

$$I_E^* = .00031$$
$$I_P^* = .2667$$
$$K_M^* = 1.033$$
$$K_P^* = 5.511$$
$$K_E^* = .01655$$
$$K_I^* = .00307$$
$$\tau_E = 35.2$$
$$\tau_I = 15.9$$

and for the governor

$$K_I = .01667$$
$$K_P = .4\left(\frac{\delta P}{90^\circ}\right)$$

These are based on I_b = 142 kg-m^2, Ω = 48 rad/sec, and N = 3 blades. The parameters for the rest of the analytical model are given in reference 1.

Figure 5 shows the variation with forward speed of the damping ratios of the three wing modes: wing vertical bending (q_1), chordwise bending (q_2), and torsion (p). Comparing the cases with and without the rotor speed governor, virtually no influence of the governor on the proprotor dynamics is observed. The governor adds a small negative real root to the system. The long time constant of this root ($\tau \cong 25 \cong 4$ revolutions) is responsible for the small effect of the governor. A greater influence is possible at low inflow (helicopter mode), where the aerodynamic damping of the rotor rotational speed is smaller.

Figure 6 shows the influence of the ψ_E and α_P degrees of freedom on the system. The engine dynamics case has the ψ_E degree of freedom, including the engine inertia and damping. The engine and transmission

dynamics case adds the Ψ_e and α_p degrees of freedom. Little influence of the engine speed perturbation and pylon roll motion on the dynamics is found, except for some coupling of these degrees of freedom with the collective rotor modes (coning and collective lag). The small role of these degrees of freedom is due to the fact they are defined not relative to space, but relative to the important motions of the system: Ψ_e is the perturbation with respect to Ψ_s, due to engine and rotor shaft flexibility; and α_p is roll of the pylon with respect to the wing tip, which is a high frequency mode. Figure 6 also shows the eingine out case, for which the engine damping is dreopped. There i little influence of the engine damping on the system dynamics.

Figure 7 compares the present model of the rotor speed dynamics with the earlier models: the windmilling case, for which the engine inertia and damping are dropped; and the constant rotor speed case, for which the Ψ_s degree of freedom is dropped entirely. The dynamics of a proprotor with a turboshaft engine are very close to the case of a windmilling rotor. There is a small influence of the engine inertia and damping on the rotor collective modes and on the Ψ_s mode, but in general the differences are not significant. On the other hand, the constant rotor speed case is not a good model for a proprotor with a turboshaft engine. As discussed in reference 1, the rotor speed perturbation has an important role in the proprotor dynamics.

Figure 8 compares the dynamics for the symmetric and antisymmetric motions of the system. In the latter case, the interconnect shaft introduces a strong spring on the rotor speed perturbation; the Ψ_s root becomes an oscillatory root with a frequency above .5/rev. The interconnect shaft has a substantial impact on the stability and gust response of the wing modes. The wing vertical bending mode (q_1) is stabilized, and the chordwise bending mode (q_2) destabilized. A similar influence is observed on the dynamics of the complete vehicle (see for example, reference 4), where typically the dynamic stability boundary is determined by an antisymmetric wing-chord

type mode. This effect of the interconnect shaft is due to the spring on the rotor speed, which changes the phasing of Ψ_s relative to the wing motion. In the q_1 mode, Ψ_s is in-phase with q_1 for the symmetric case, but lags q_1 by about 90° for the antisymmetric case. In the q_2 mode, Ψ_s lags q_2 by about 60° for the symmetric case, and is 180° out-of-phase with q_2 for the antisymmetric case. There is little influence of the interconnect shaft on the rotor modes in general. The gust response of Ψ_s is actually somewhat lower for the antisymmetric case. However, for the antisymmetric case the Ψ_s motion produces drive-train loads, which may be significant; indeed typically the design limit drive-train loads are due to antisymmetric longitudinal gusts.

CONCLUSIONS

In summary, there is some influence of the engine inertia and damping on the proprotor dynamics, little influence of the governor, and little influence of the engine speed or pylon roll degrees of freedom. The dynamic behavior of a proprotor with a turboshaft engine is very close to the case of a windmilling rotor. The interconnect shaft has a large and important effect on the dynamics for antisymmetric motion of the proprotor.

On the basis of the present results and those of reference 1, we conclude that the rotor model required for an analysis of proprotor dynamics consists of the following degrees of freedom: the first two bending modes and the rigid pitch mode per blade; gimbal pitch and roll for the gimballed rotor; and the rotor speed degree of freedom including the engine inertia and damping effects. This is a nine degree-of-freedom model; in some cases it may be reduced to six degrees of freedom by using the quasistatic-torsion approximation, as discussed in reference 1. The rotor speed governor can be included for completeness; it does not add any degrees of freedom to the model.

REFERENCES

1. Johnson, Wayne, "Analytical Modeling Requirements for Tilting Proprotor Aircraft Dynamics," NASA TN D-8013, January 1975

2. Johnson, Wayne, "Dynamics of Tilting Proprotor Aircraft in Cruise Flight," NASA TN D-7677, May 1974

3. Johnson, Wayne, "Analytical Model for Tilting Proprotor Aircraft Dynamics, Including Blade Torsion and Coupled Bending Modes, and Conversion Mode Operation," NASA TM X-62369, August 1974

4. Edenborough, H. Kipling; Gaffey, Troy M.; and Weiberg, James A.; "Analyses and Tests Confirm Design of Proprotor Aircraft," AIAA Paper No. 72-803, August 1972

5. Ashley, Holt, Engineering Analysis of Flight Vehicles, Addison-Wesley Publishing Company, Reading, Massachusetts, 1974

6. Hill, Philip G. and Peterson, Carl R., Mechanics and Thermodynamics of Propulsion, Addison-Wesley Publishing Company, Reading, Massachusetts, 1965

TABLE 1.

Eigenvalues and Gust Response at V = 250 knots.

	Engine	Engine with Governor	Engine/ Inter-connect Shaft	Engine/ Transmission	Engine/ Transmission with Governor	Engine/ Transmission Inter-connect Shaft	Windmilling	Engine out
Eigenvalues (dimensionless, based on Ω = 48 rad/sec)								
ζ_β mode	−.338	−.297	−.224±i.560	−.341	−.300	−.230±i.543	−.434	−.328
ζ_ζ mode	-	-	-	−.160±i1.941	−.160±i1.941	−.059±i2.376	-	-
ω_β mode	-	-	-	−.379±i6.921	−.380±i6.923	−.379±i6.921	-	-
governor	-	−.0395	-	-	−.0395	-	-	-
Gust Response (dimensionless and normalized)*								
wing tip vertical acc. ($\ddot{q}_1$)	.0484	.0495	.0371	.0484	.0495	.0372	.0507	.0448
wing tip chordwise acc. ($\ddot{q}_2$)	.0208	.0211	.0152	.0210	.0213	.0150	.0195	.0218
wing torsion acc ($\ddot{p}$)	.118	.118	.114	.124	.124	.114	.115	.110
rotor coning (β_0)	.051	.051	.092	.051	.050	.092	.049	.054
rotor flapping (β)	1.762	1.762	1.738	1.762	1.763	1.738	1.767	1.671
rotor collective lag (ζ_0)	.108	.112	.603	.112	.116	.603	.056	.118
rotor cyclic lag (ζ)	.852	.853	.787	.851	.852	.787	.866	.796
rotor collective torsion (θ_0)	.042	.440	.143	.042	.440	.143	.038	.041
rotor cyclic torsion (θ)	.769	.769	.745	.769	.769	.745	.774	.693
rotor speed perturbation (Φ_x)	1.245	1.276	1.074	1.244	1.266	1.294	1.293	1.379

*Dimensional values are not given since only the comparison between the cases is of concern here; study of the actual gust response level is left to another report.

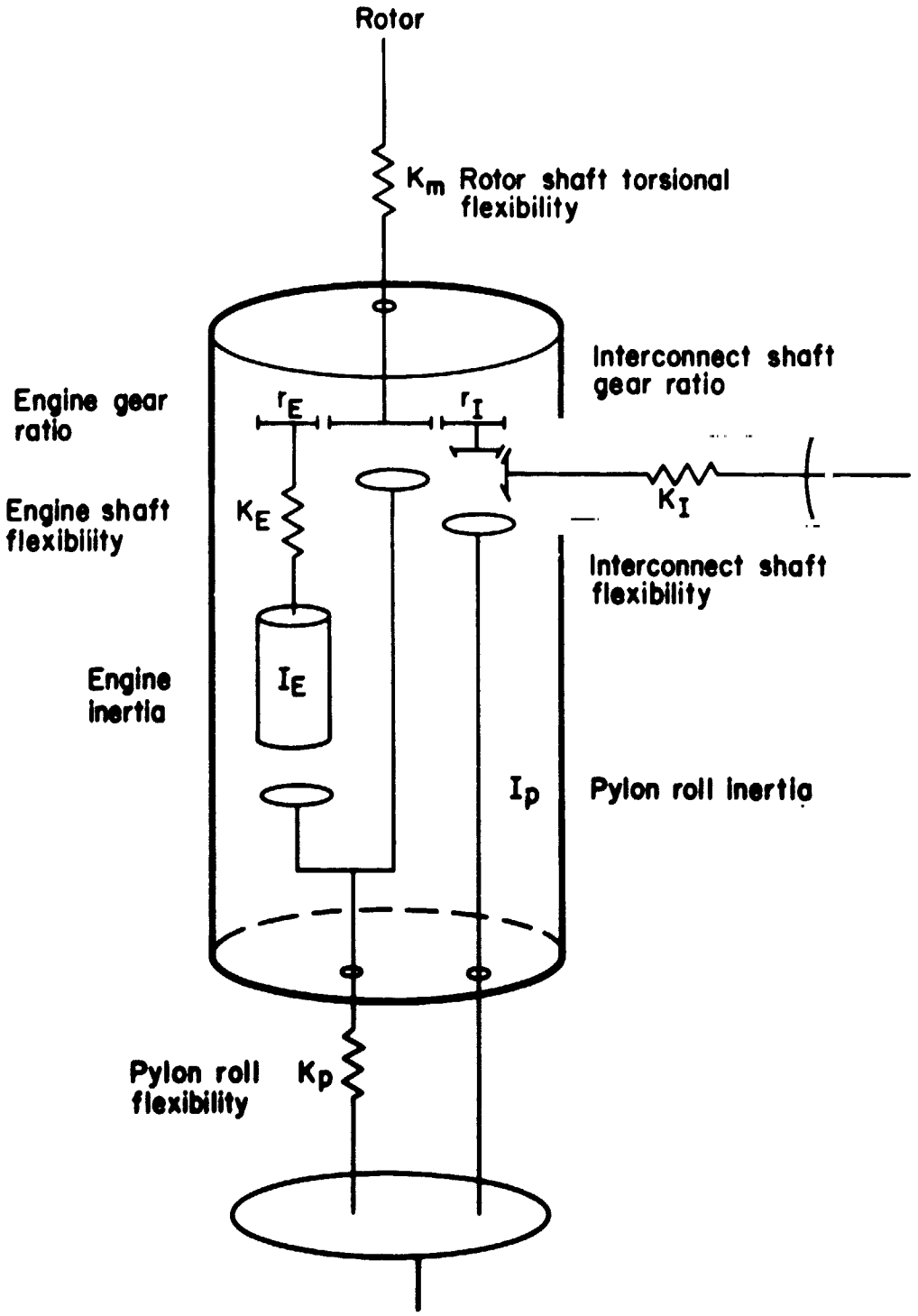

Figure 1. Schematic of proprotor transmission, engine, and interconnect shaft.

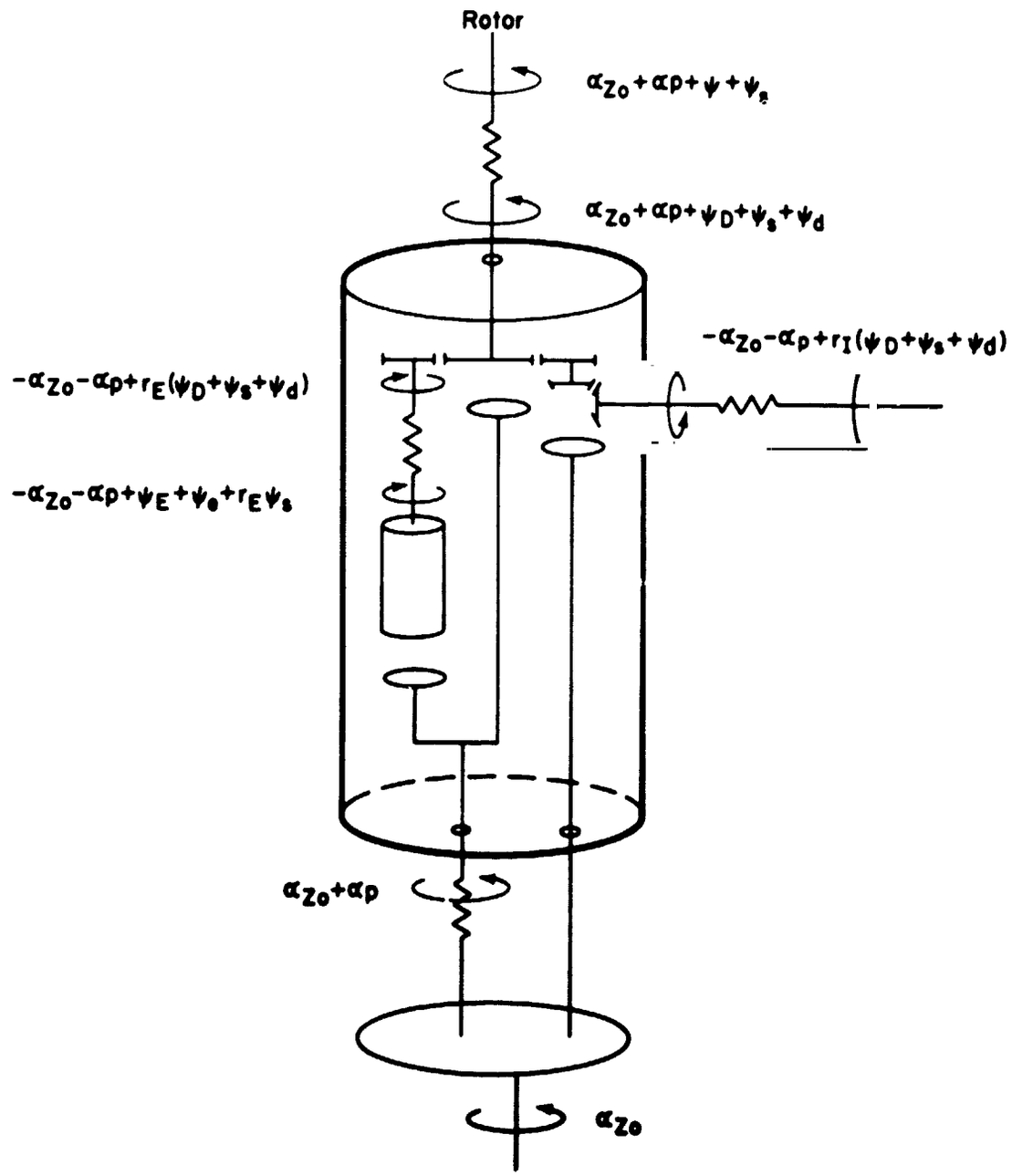

Figure 2. Definition of rotations in engine/transmission model.

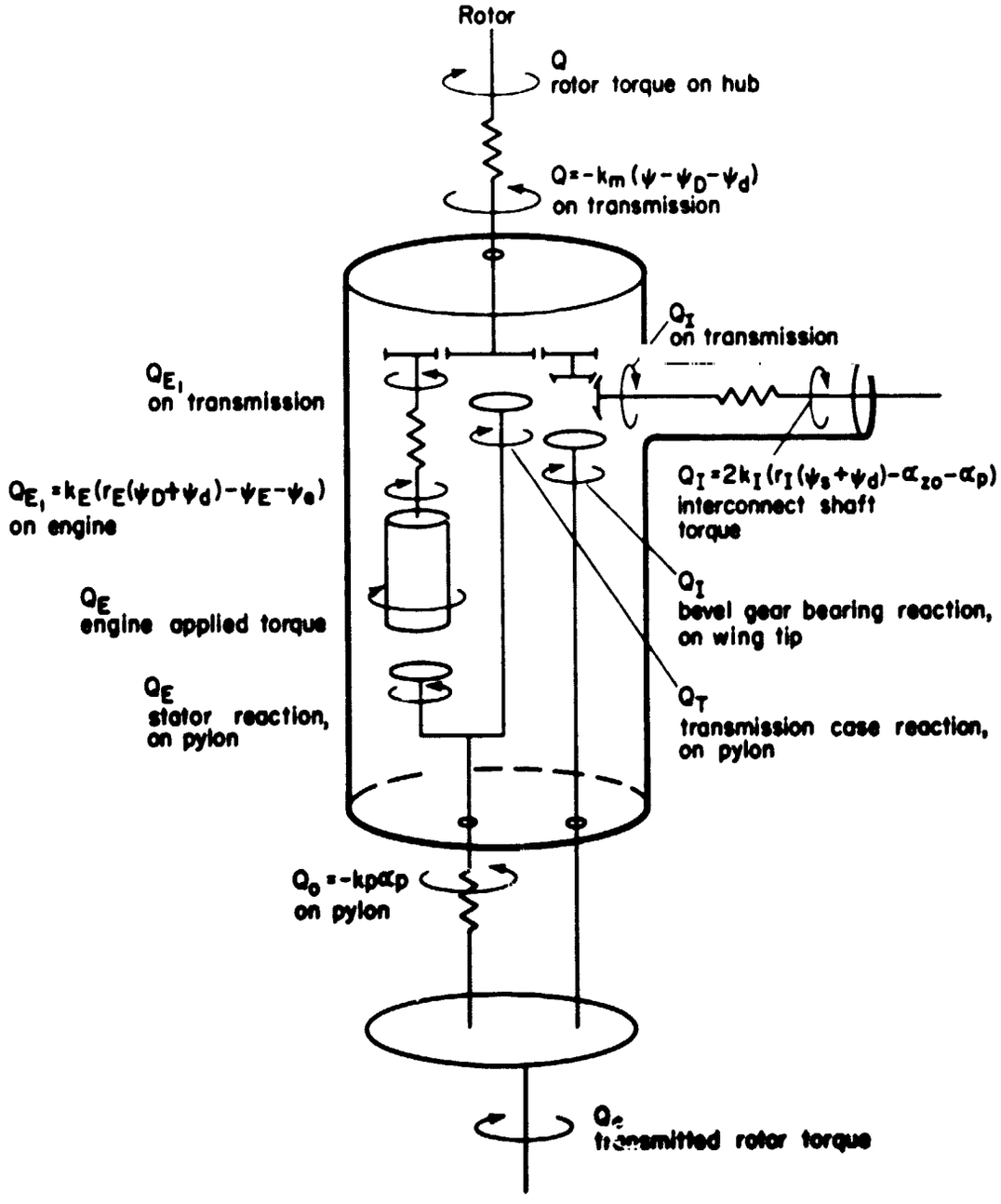

Figure 3. Definition of torques in engine/transmission model.

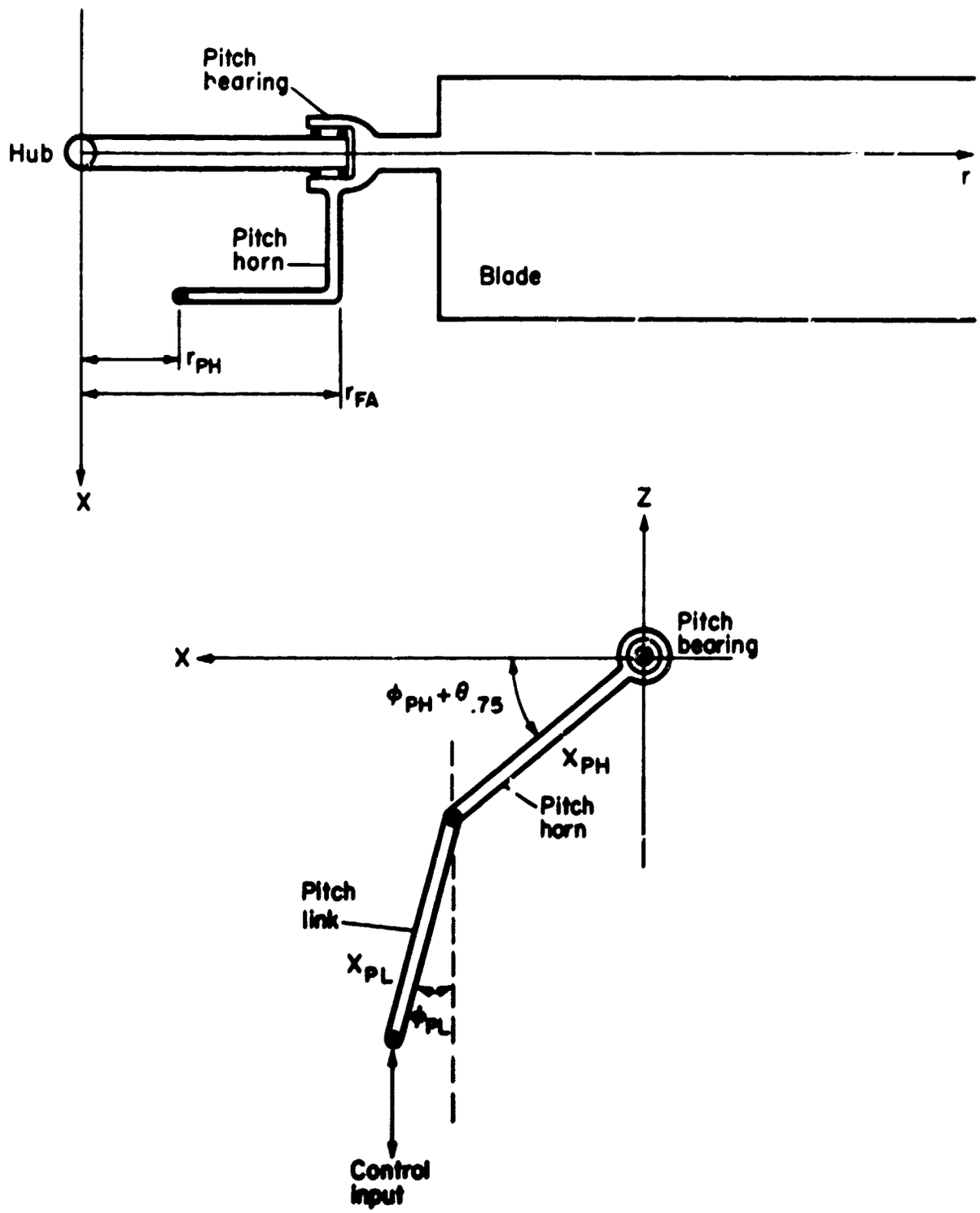

Figure 4. Schematic of blade root and control system geometry for calculating the kinematic pitch/bending coupling.

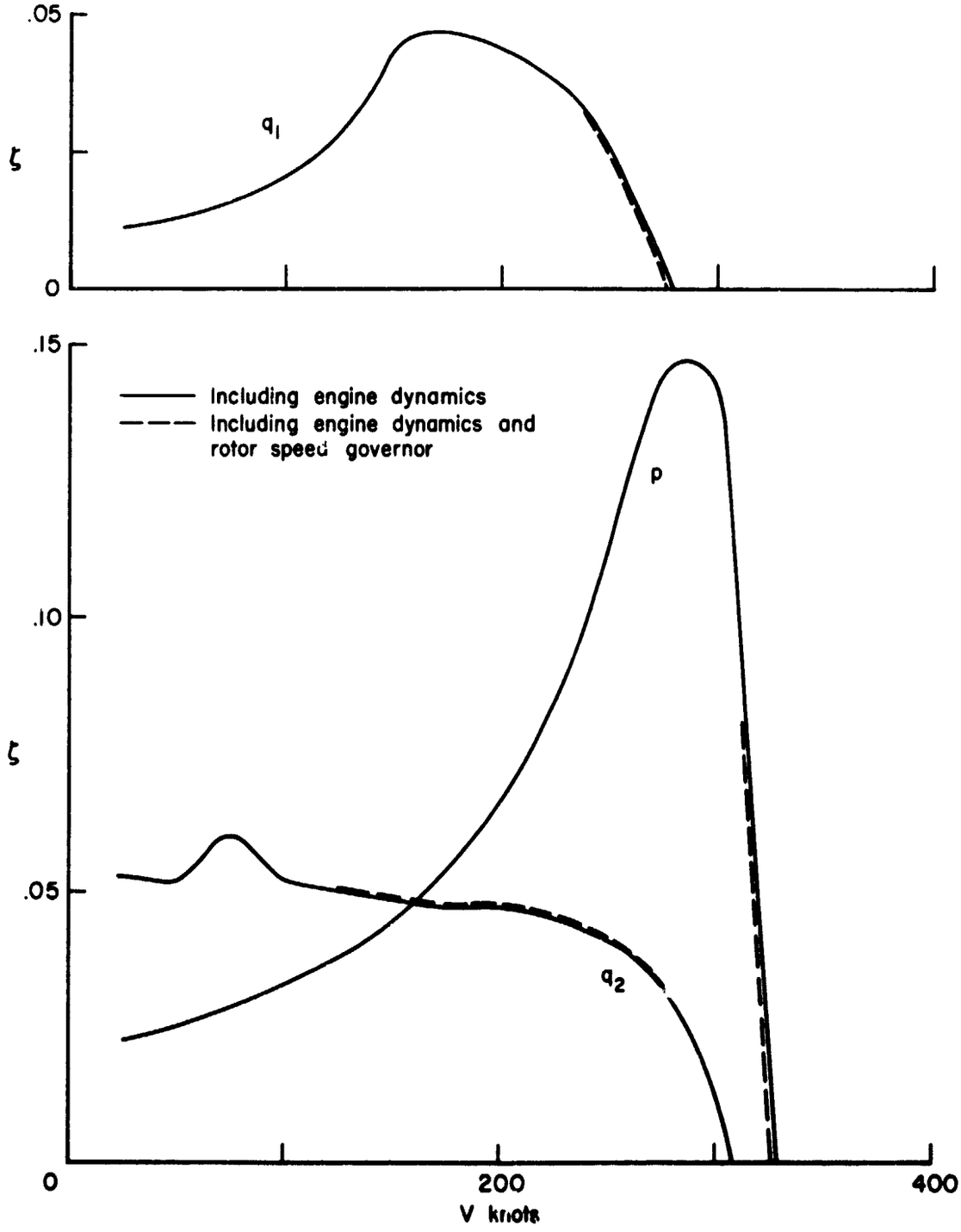

Figure 5. Wing mode damping ratios as function of forward speed, for gimballed proprotor and cantilever wing in cruise mode; including engine dynamics, with and without rotor speed governor; q_1 is the wing vertical bending, q_2 the wing chordwise bending, and p the wing torsion.

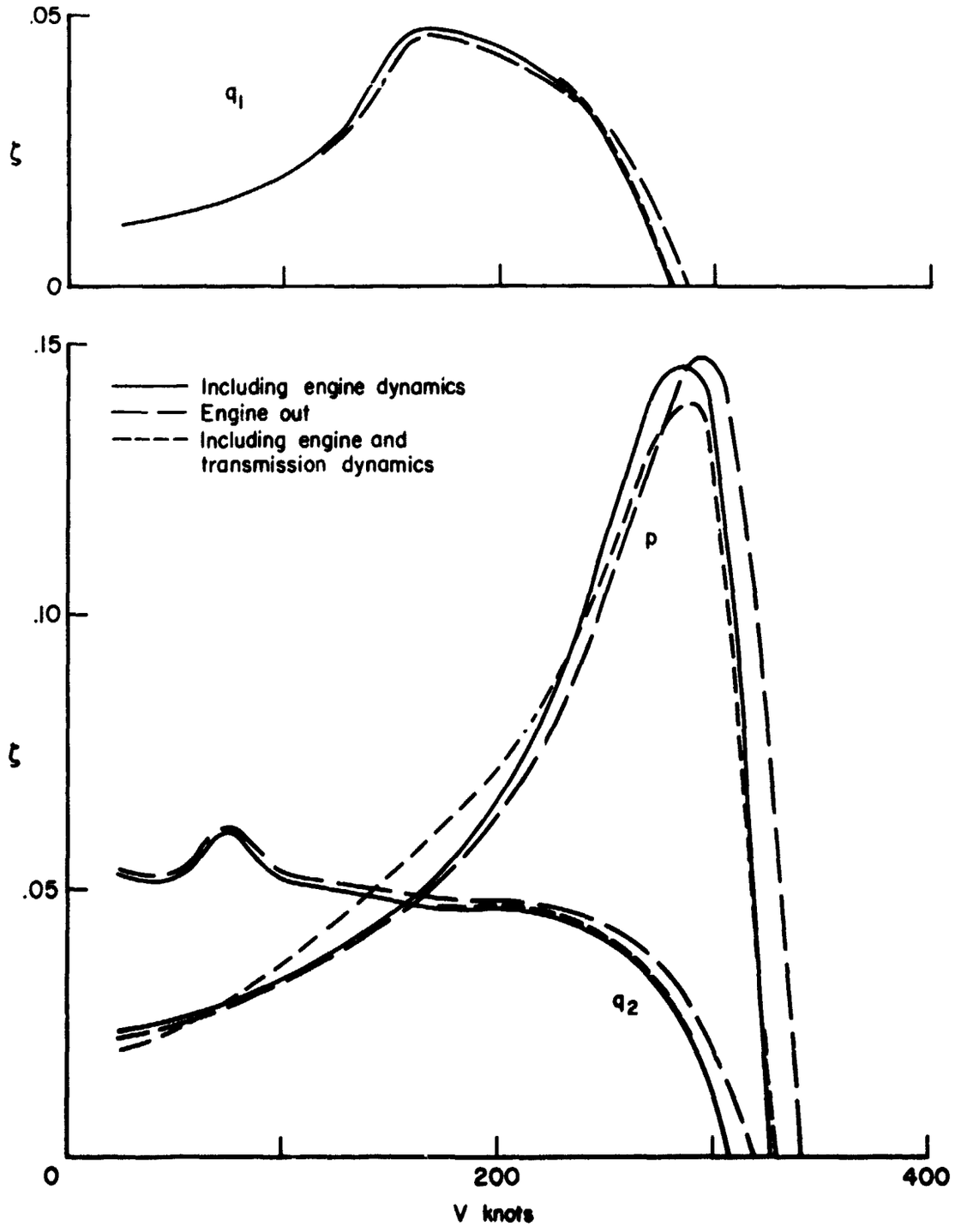

Figure 6. Wing mode damping ratios for gimballed proprotor, showing influence of engine and transmission dynamics ($\Delta\varphi_e$ and α_p degrees of freedom included), and engine damping (absent for engine out case).

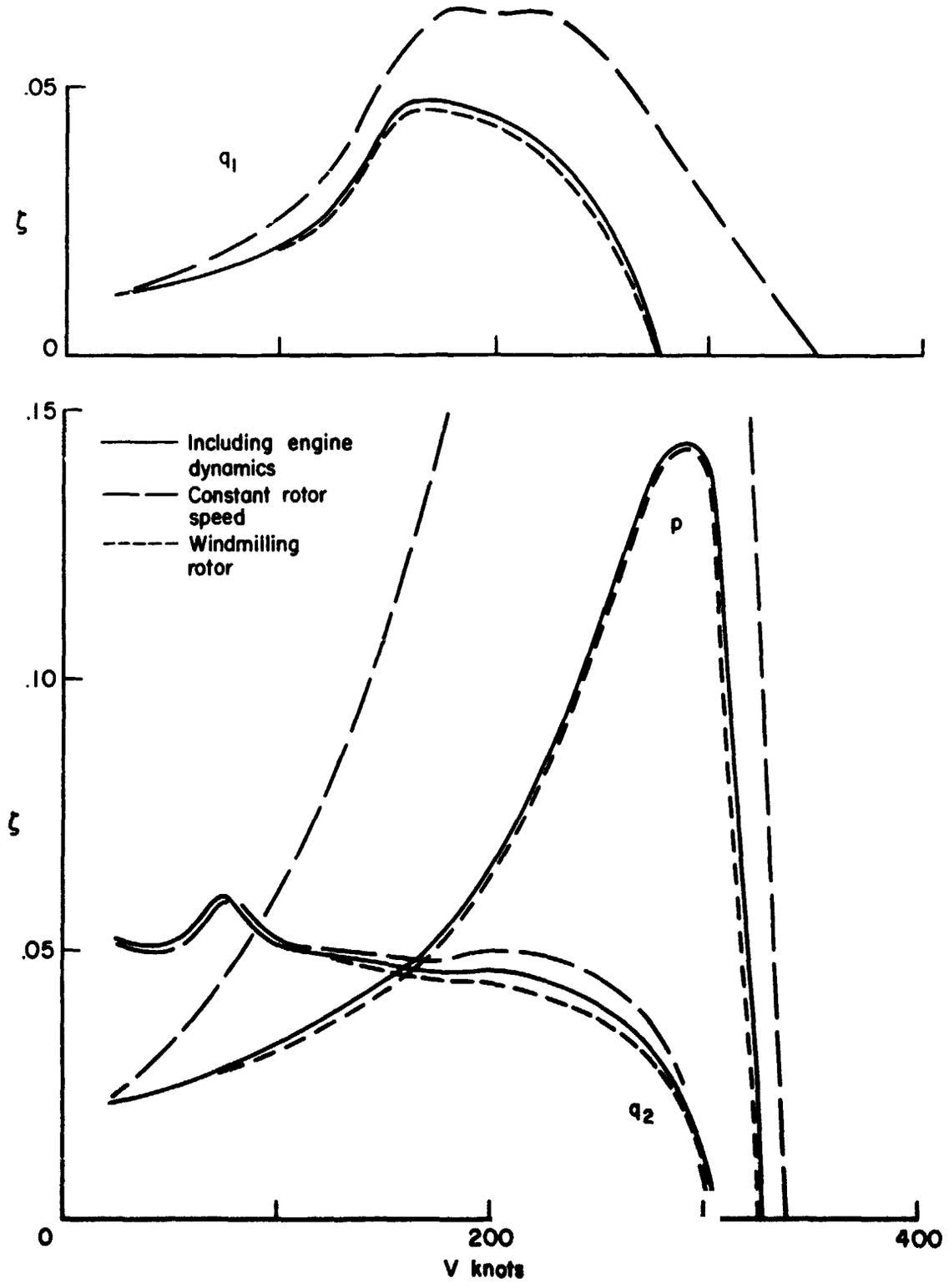

Figure 7. Wing mode damping ratios for gimballed proprotor, comparing windmilling and constant rotor speed cases with model including engine dynamics.

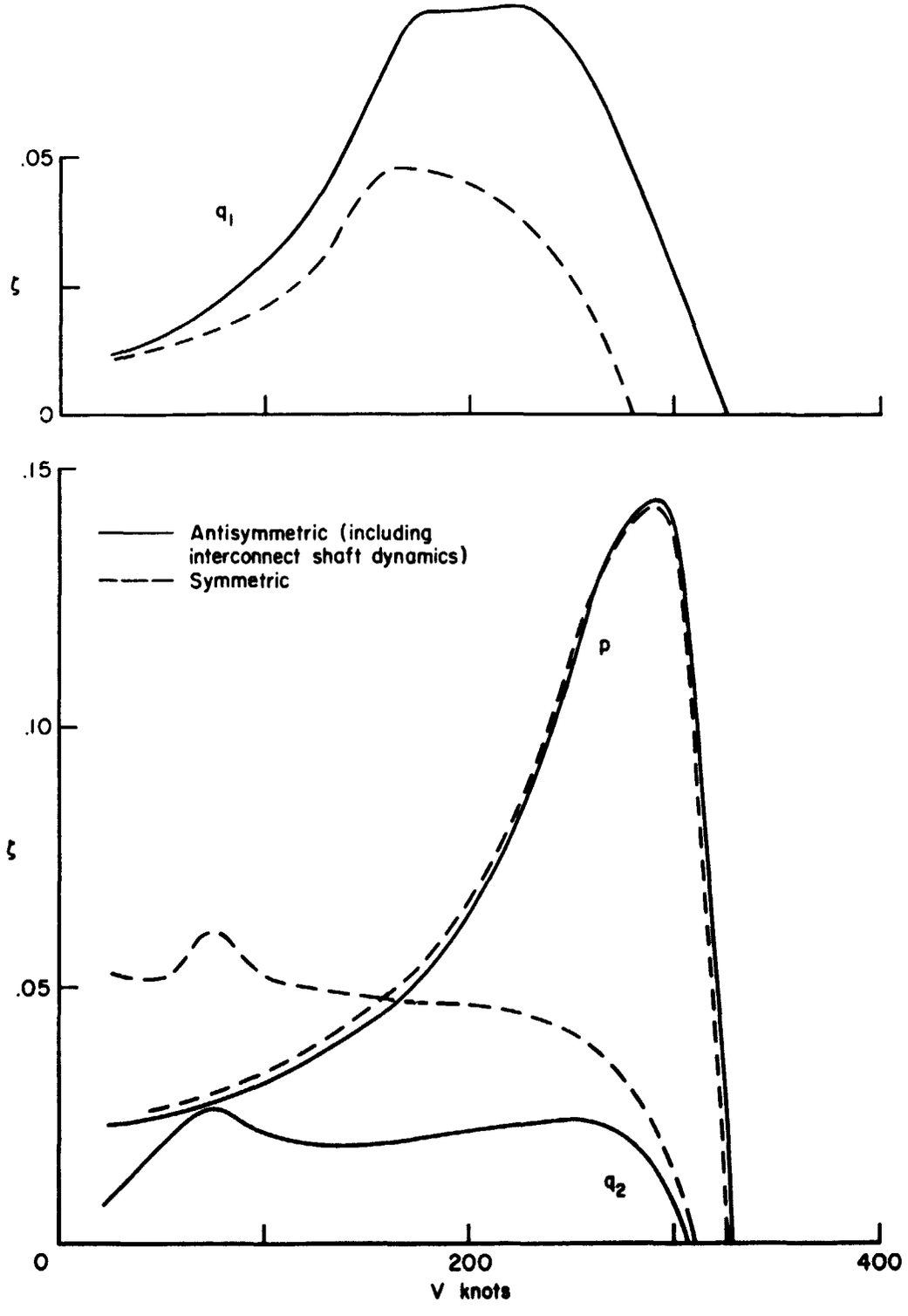

Figure 8. Wing mode damping ratios for gimballed proprotor, for symmetric and antisymmetric motion; the latter case includes the interconnect-shaft influence.